ST2 to Top mass feedforward control at 0.1 Hz

Edgard Bonilla

June 27, 2018

Why do we want to use feedforward?

The reason can be found in the SEI log 1237. Conor Mow-Lowry showed that there is correlation between the DARM projected suspension point motion for the quadruple suspensions around 0.1 Hz, as evidenced by the coherence plot of these signals 1. In that same post, shows that if we performed a perfect coherent subtraction of that signal we could get a factor of 3 reduction of the overall RMS velocity for the gravitational wave channel (DARM).

In practice, we can take the suspension point longitudinal motion from the GS13 geophones and either subtract it locally at each QUAD or project these signals into the DARM degree of freedom and subtract it at a particular suspension. In both cases the subtraction would be performed by actuating at the top stage of the suspension system. Most of the calculations done in this document assume that the local actuation scheme is the one we want to utilize.

This document attempts to summarize the ideas and findings we had while analyzing the viability of this plan. We will start by briefly describing the theoretical estimates done by using the QUAD model, which sets bounds on the tolerances needed for the control scheme to work. Next, we show that this approach is viable during the normal operation of the interferometer by comparing transfer function measurements from O2. Lastly, we dive into the details for the implementation of the control filters withing the real time models used at the sites.

1 Calculations using the QUAD model

We used the QUAD model to estimate the effect of a feedforward filter that uses the Suspension point GS13 signal and actuates on the top stage of the quadruple suspension. Every single plot uses the ASD for the ground motion taken from a earthquaque and incident free time, together with a model of the GS13 sensor noise. Figure 2 shows the input signals for this analysis, we can see that the signal to noise ratio in the 50 - 600 mHz frequency band is high enough that we could make improvements using feedforward. However, in principle, we would like to stay away from the resonances of the quadruple suspensions, that is, below 400 mHz.

The result of this preliminary analysis is that we could, in principle get a significant reduction of the test mass displacement around 100 mHz by applying feedforward control from the suspension point longitudinal displacement, to the top mass longitudinal and pitch motions. It is important to highlight that we

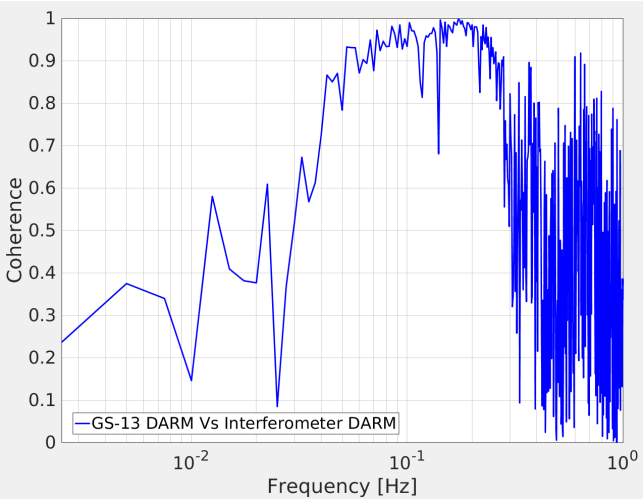

Figure 1: Coherence between the DARM projected suspension point signal as measured by the GS13 and the interferometer's DARM signal. We attempt to use feedforward in the band where the coherence is ≈ 1

need to actuate the longitudinal and pitch degrees of freedom simultaneoustly. If we ignore the cross coupling between these degrees of freedom, we would induce a DC pitch on the test mass that could compromise the performance of the interferometer. This result can be appreciated in Figures 3a and 3b.

1.1 Shape for the theoretical filters

The feedforward filters that need to be applied to get the performance shown in Figure 3 are constants. This result is to be expected from a multi stage pendulum built like the quadruple suspensions, given that we are trying to simultaneously cancel the effect from the suspension point Longitudinal motion into both the Longitudinal and pitch degrees of freedom of the top mass.

The Length to Length filter works as a spring constant κ, dominated by the pendulum's sttiffness: $\kappa \approx \frac{gM}{L_{\text{top}}}$, where M is the mass of the quadruple pendulum, L_{top} is the vertical distance between the suspension point and the attachment point of the wires to the top mass. The value found in the QUAD model is 2864 N/m, the approximate value is 2844 N/m.

The Length to Pitch filter proportional the torque exerted by that spring on the top mass. So it is κl with l being an effective lever arm term. This term can be found as the distance between the center of mass and attachment point of the wires of the top mass. In the current iteration for the QUAD Matlab model $l = 1.36$ mm

Ideas about how to approximate these numbers for the real apparatus are given in the 'Implementation' section of this document.

1.2 Projected Tolerance for the filters

The most delicate part to get right when using the Feedforward scheme is going to be the lever arm term l. Since its scale is small and its effect on the Pitch

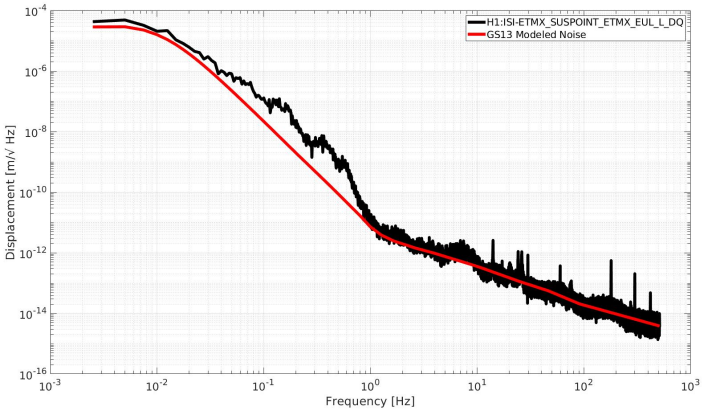

Figure 2: Input signals for the feedforward modeling. The ground mottion is from August 4 2017, 12:00 UTC. The GS13 sensor noise was modeled using the `SEI_sensor_noise.m` script from the seismic SVN and adding 4 real poles at 10 mHz, in accordance with the calibration described in the Hanford aLog 4553

motion of the top mass is significant. Figure 4 indicates that we can comfortably aim to approximate l to within 10% accuracy ($\Delta l = \pm 136 \mu$m) while keeping the cross coupling to test mass pitch motion low between 0.1 and 0.3 Hz. We could then get rid of the low frequency coupling by using a high pass filter. Preliminary analysis (SEI Log 1325) suggests that this accuracy is enough.

It is important to note though, that we have reasons to believe that the relevant figure for this approximation is not the percent error but the absolute value of the lever arm in μm. However we

In order for the feedforward scheme to be robust, we need to make sure we can approximate l to within 100μm during the normal interferometer operation. The details about how likely it is that we could do that are fleshed out in the next section.

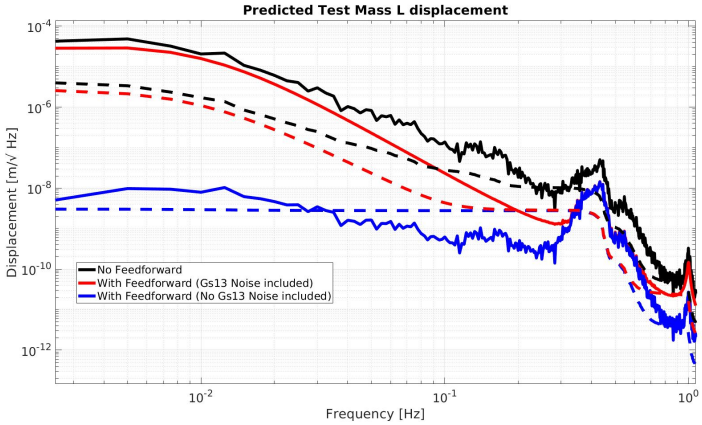

(a) Effect of the Suspension point to top mass feedforward filter on the test mass Longitudinal displacement. The dashed lines correspond to the integrated RMS displacements for the corresponding traces.

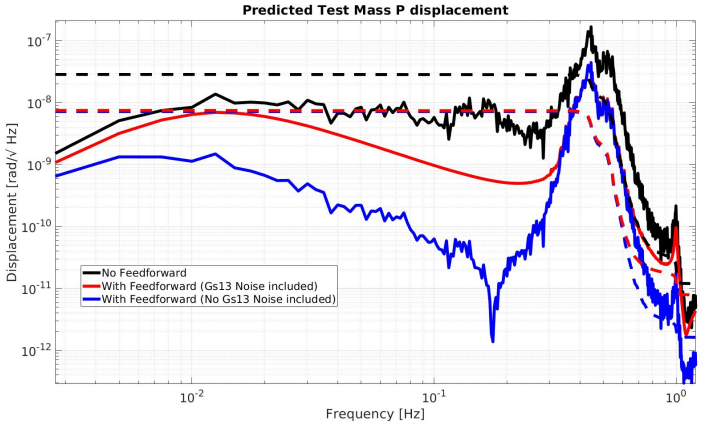

(b) Effect of the Suspension point to top mass feedforward filter on the test mass Pitch displacement. The dashed lines correspond to the integrated RMS displacements for the corresponding traces.

2 Viability in the real system

2.1 Measurements from H1 ITMX and ITMY during O2

The results from this section can be found in more detail in th SEI logs, the figures appear in the second appendix. The figures show the top mass longitudinal-pitch cross couplings at the top mass level. Here we show the measurements corresponding to O2 only, all of them are made in vacuum and the Seismic system was in the 'Isolated' state during the measurement.

The most important feature that we want to note is that the cross coupling transfer functions are not reciprocal. In fact, for H1 ITMY these two terms don't even have the same phase at DC. This implies that there must be some systematic problem either in the way we actuate the system or the intepretation of the measured quantities. This is further explored in the second appendix of

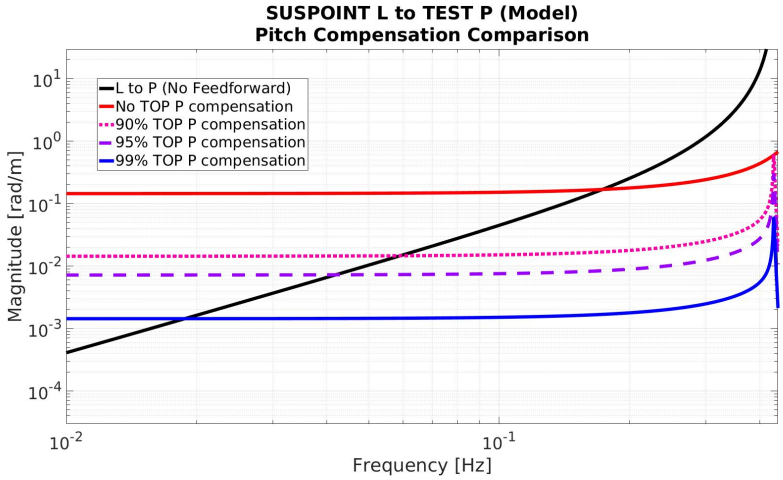

Figure 4: Suspension point Longitudinal displacement to test mass displacement transfer function as modeled by the QUAD model. The different traces represent different tolerances on the feedforward filter's lever arm term l.

this document, without a satisfying conclusion. For now we will focus on the O2 measurements.

As an estimate, we take a look at the dispersion between all of the lever arm factors corresponding to the cross coupled transfer functions at low frequencies, by using the equation $l = \lim_{f\to 0} \frac{T_{PL}}{T_{PP}}$, where T_{PP} and T_{PL} are the top mass to top mass pitch to pitch and length to pitch transfer functions, respectively. Δl is calculated as the half difference between the maximum and minumum values for the lever arm factors.

$$\text{ITMX:} \qquad \bar{l} = -9600\mu\text{m} \quad , \quad \Delta l = 1200\mu\text{m} \quad , \quad \frac{\Delta l}{|l|} = 12.5\% \tag{1}$$

$$\text{ITMY:} \qquad \bar{l} = 2670\mu\text{m} \quad , \quad \Delta l = 280\mu\text{m} \quad , \quad \frac{\Delta l}{|l|} = 10.5\% \tag{2}$$

Both of the lengths are close to the desired 10% accuracy level, although they are significantly bigger than the cross coupling expected by the matlab model. We need to investigate this further, since the lack of reciprocity of the transfer function measurements can change how significant the absolute error is compared to the percent error on l.

2.2 Estimates for actuator misalignment

The effects of actuator misalignment are approximated to first order by using a simple model that assumes the magnet can be treated as a dipole. The full mathematical treatment for this is laid out in the first appendix of this document.

2.2.1 Sagging due to Temperature

Lowering the top mass by a distance ΔV relative to the cage, generates excess torque in the pitch degree of freedom when actuating in the longitudinal

direction. The magnitude of the torque is given by:

$$\Delta\tau = |F|\frac{|\Delta V|}{2} \tag{3}$$

Which is equivalent to a Δl of $\frac{|\Delta V|}{2}$. Brett Shapiro calculated the suspension sagging due to temperature to be 108 μm/^{o}C (Caltech aLog 12581). If we go with our stringent estimate of $\Delta l \leq 100$ μm, that leaves us with 2 degrees Celsius of tolerance to temperature variation. This requirement is satisfied by the current facilities. Not though, that this is not enough to explain either the values for Δl from O2 presented before.

2.2.2 ST2 DC pitch

3 Implementation

3.1 Modifications to the models

In terms of implementation, we need to make four modifications to Quadruple suspensions master model. These are:

1. Add two filter blocks to do feedforward. The inputs are the signals from suspension point Longitudinal and Pitch motion (as measured from the GS-13), respectively. The outputs are a Length and Pitch compensation at the top mass. These blocks and inputs need to be added both to M0 and R0.

2. Modify the 'Add' blocks for M0 and R0 to accomodate the new inputs.

3.2 Tuning and testing

The feedforward path should be turned on after the seismic system is in the 'Isolated' mode, to increase the reliability of the cross coupling lever arm factor l. We should be on this mode before we start estimating the feedforward constants κ and l.

It is better to start by estimating the lever arm factor l. We could take Top Mass to Top Mass Longitudinal (L) and Pitch (P) transfer functions. Estimating the tuning by using $l = \lim_{f\to 0} \frac{T_{PL}}{T_{PP}}$.

The next step is to find κ. We can estimate κ by dividing the ST2 X to Top Mass L transfer function by the Top Mass L to L transfer function at low frequencies.

Alternatively, we can start by estimating $\kappa \approx \frac{gM}{L_{\text{top}}}$ and tune by repeatedly taking the ST2 X to Top Mass L transfer function, stopping when this function gets close to -1. In this case, the OSEM should register the motion of the cage, but no signal from the top mass.

To establish the periodicity of this tuning procedure, more tests will be required, as well as more input from the opperators and staff at the sites. One idea is to look at the coherence between the DARM projected GS-13 motion for the suspension points and both DARM and DHARD. The former gives more information about κ being well tuned, and the latter about l. When both of these coherences are below 50% at around 0.1 Hz, then we can stop tuning.

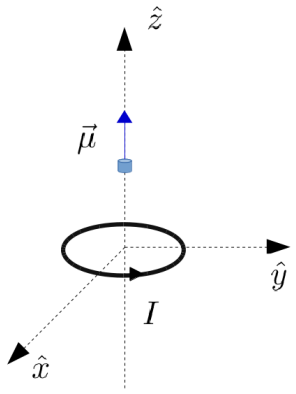

Figure 5: Simplified model for a magnet and an OSEM coil. The magnet is modeled as a magnetic dipole $\vec{\mu}$ aligned with the axis of symmetry of the coil. We frame all results on the reference frame of the coil.

4 Appendix: Estimating Error due to Actuator misalignment

We can approximate the interaction of an OSEM coil with a magnet as the interaction of a current loop with a magnetic dipole $\vec{\mu}$. The magnetic field of a current loop carrying a current I on its axis of symmetry is given by:

$$\vec{B}(0,0,z) = \frac{\mu_0 I}{2} \frac{R^2}{(z^2+R^2)^{3/2}} \hat{z} \tag{4}$$

The force and torque on a magnetic dipole are given by:

$$\vec{F} = \nabla(\vec{\mu} \cdot \vec{B}) \quad , \quad \vec{\tau} = \vec{\mu} \times \vec{B} \tag{5}$$

Nominally, the magnet and coil of an OSEM are aligned, so that $\vec{\mu}$ is aligned with the axis of symmetry of the coil. In this case the force on the magnet is only on the $\hat{z}$ direction and it is given by:

$$\vec{F} = \mu \frac{\mu_0 I}{2} \frac{-3zR^2}{(z^2+R^2)^{5/2}} \hat{z} = \mu \frac{-3\mu_0 I}{2R^2} \frac{\alpha}{(1+\alpha^2)^{5/2}} \hat{z} \tag{6}$$

Where $\alpha = z/R$ is a normalized distance from the axis, since the radius of the coil is the relevant physical scale for the system. Since μ and $\vec{B}$ are parallel, the torque on the dipole is zero.

Moving forward, it will be useful to define the on axis magnetic field B_0 and force F_0 on a dipole placed at a distance z from the center. These two are related by‘:

$$F_0 = \frac{-3\alpha}{1+\alpha^2} \frac{\mu}{R} B_0 \tag{7}$$

We will use these as references when estimating errors due to misalignment of the magnet with respect to the coil.

Since we will be making linear approximations, we will treat each magnet displacement independently and then sum the effects to get the overall error estimate.

4.1 Axis of symmetry displacement dz

For an infinitesimal displacement along the axis of symmetry, the magnetic dipole will not suffer any torque, however. There is going to be a change in the force exerted by the magnet. Using $\vec{B}(0,0,z+dz) \approx \vec{B_0} + \frac{\partial B_z}{\partial z} dz\hat{z}$ we find:

$$\vec{F}_{dz} = \vec{F}_0 + \mu dz \nabla \left(\frac{\partial B_z}{\partial z} \right) \tag{8}$$

Now, from $\nabla \times \vec{B} = 0$ (which is valid everywhere except for the current loop) we know $\frac{\partial B_z}{\partial x} = \frac{\partial B_x}{\partial z}$. Since B_x is identically zero all along the axis of symmetry of the loop: $\frac{\partial^2 B_z}{\partial x \partial z} = \frac{\partial^2 B_x}{\partial z^2} = 0$. A similar argument can be made for the y-direction derivative. Finally:

$$\vec{F}_{dz} = \vec{F}_0 + \mu dz \frac{\partial^2 B_z}{\partial z^2} \hat{z} \tag{9}$$

as we would expect from a heuristic approach. Now, in our α notation:

$$\frac{\partial^2 B_z}{\partial^2 z} = \frac{-3\mu_0 I}{2R^3} \frac{1-4\alpha^2}{(1+\alpha^2)^{7/2}} = \frac{1}{R} \frac{1-4\alpha^2}{\alpha(1+\alpha^2)} \frac{F_0}{\mu} \tag{10}$$

One important thing to note is that if we place the magnetic dipole at $\alpha = 1/2$, at half the radius of the coil away from it, this second derivative term is zero, this should be the case for the OSEMs, but we are going to keep it for completeness' sake.

4.2 Angular displacement $d\theta$

Without loss of generality, let's assume that the magnetic moment $\vec{\mu}$ is rotated by a small angle $d\theta$ so that it has a small component on the $\hat{x}$ direction, but remains on the axis of symmetry. In that case:

$$\vec{F}_{d\theta} = \nabla \left(\vec{\mu} \cdot \vec{B} \right) = \mu \nabla \left(B_z + B_x d\theta \right) \tag{11}$$

This equation contains the derivatives of B_x and B_z with respect to every coordinate axis. We can simplify it by considering symmetry and Maxwell's equations:

- From the symmetry of the problem, we know that the magnitude of z component of the magnetic field is maximum on the axis of symmetry, so $\frac{\partial B_z}{\partial x} = \frac{\partial B_z}{\partial y} = 0$ in the axis of symmetry.
- From $\nabla \cdot \vec{B} = 0$ and a symmetry argument we can deduce that $\frac{\partial B_x}{\partial x} = -\frac{1}{2}\frac{\partial B_z}{\partial z}$
- From the symmetry of the problem, we know there is no magnetic field in de azimuthal direction. More specifically, $B(x=0,y,z) = 0$ for all (y,z). This implies $\frac{\partial B_x}{\partial y} = \frac{\partial B_x}{\partial z} = 0$ in the (y,z) plane

These considerations help simplify the equation for the force on this misaligned magnet to:

$$\vec{F}_{d\theta} = \mu \left(-\frac{1}{2} \frac{\partial B_z}{\partial z} d\theta \hat{x} + \frac{\partial B_z}{\partial z} \hat{z} \right) = \left(-\frac{1}{2} d\theta \hat{x} + \hat{z} \right) F_0 \tag{12}$$

On the other hand, the torque exerted by the magnetic field will be given by:

$$\vec{\tau}_{d\theta} = \mu B_0 d\theta(\hat{x} \times \hat{z}) = -\frac{1}{3}\left(\alpha + \frac{1}{\alpha}\right) RF_0(\hat{x} \times \hat{z}) \tag{13}$$

$$\vec{\tau}_{d\theta} = \left[-\frac{1}{3}\left(\alpha + \frac{1}{\alpha}\right) Rd\theta\right] \hat{x} \times \vec{F}_0 \tag{14}$$

4.3 Off-axis displacement dx

Without loss of generality, let's assume that the magnet moves relative to the coil in the $\hat{x}$ direction, but keeping its magnetic moment aligned with the z axis. Using the approximation $\vec{B}(dx, 0, z) = \vec{B}_0 + \frac{\partial \vec{B}}{\partial x} dx$ we find a force

$$\vec{F}_{dx} = \vec{F}_0 + \mu dx \nabla \left(\frac{\partial B_z}{\partial x}\right) \tag{15}$$

Similar to what we did before, we will simplify this equation by using symmetry arguments and Maxwell's equations:

- From $\nabla^2 \vec{B} = \nabla\left(\nabla \cdot \vec{B}\right) - \nabla \times (\nabla \times \vec{B}) = 0$ and symmetry we can find that $\frac{\partial^2 B_z}{\partial x^2} = -\frac{1}{2}\frac{\partial^2 B_z}{\partial z^2}$ on the z axis.
- From $\nabla \times \vec{B} = 0$, we get $\frac{\partial^2 B_z}{\partial y \partial x} = \frac{\partial^2 B_x}{\partial z \partial y}$, which is zero in the axis of symmetry.
- $\frac{\partial B_z}{\partial x} = 0$ for all z in the axis of symmetry. In consequence, $\frac{\partial^2 B_z}{\partial z \partial x} = 0$

$$\vec{F}_{dx} = \vec{F}_0 + \mu dx \nabla \left(\frac{\partial B_z}{\partial x}\right) \tag{16}$$

With all of these in mind, we obtain:

$$\vec{F}_{dx} = \vec{F}_0 - \frac{1}{2}\mu dx \frac{\partial^2 B_z}{\partial z^2} \hat{z} \tag{17}$$

For the torque, we note that since $\nabla \cdot \vec{B} = 0$ and $x - y$ symmetry imply $\frac{\partial B_x}{\partial x} = -\frac{1}{2}\frac{\partial B_z}{\partial z}$. And so:

$$\vec{\tau}_{dx} = \mu \hat{z} \times \left(\frac{\partial B_x}{\partial x} dx \hat{x}\right) = \left[\frac{1}{2} dx\right] \hat{x} \times \vec{F}_0 \tag{18}$$

5 Appendix: On the Longitudinal to Pitch Coupling at the Top Mass

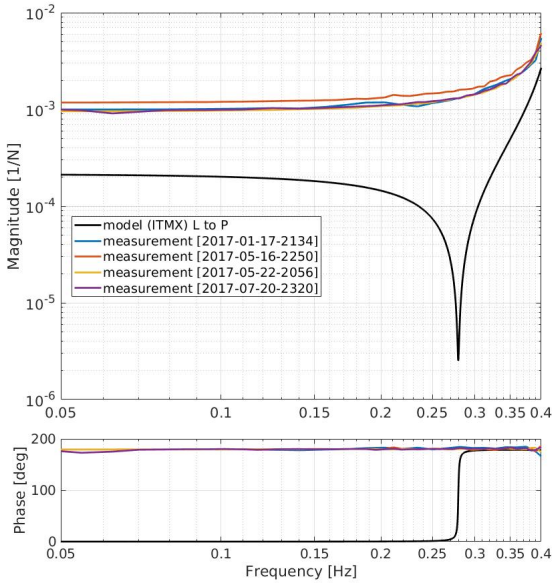

(a) H1 ITMX Top Mass Longitudinal to Top Mass Pitch transfer functions at different times during O2. Note that the measurements average aroun -10^{-3} [1/N]

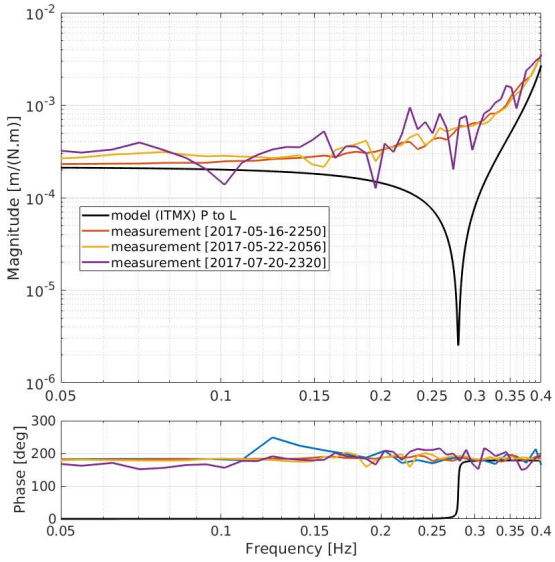

(b) H1 ITMX Top Mass Pitch to Top Mass Longitudinal transfer functions at different times during O2. Note that the traces average around -3×10^{-4} [1/N]

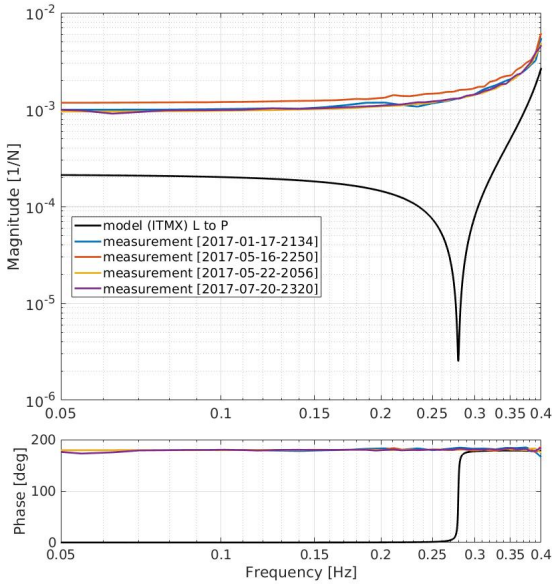

(a) H1 ITMY Top Mass Longitudinal to Top Mass Pitch transfer functions at different times during O2. Note that the measurements average aroun 2×10^{-4} [1/N]

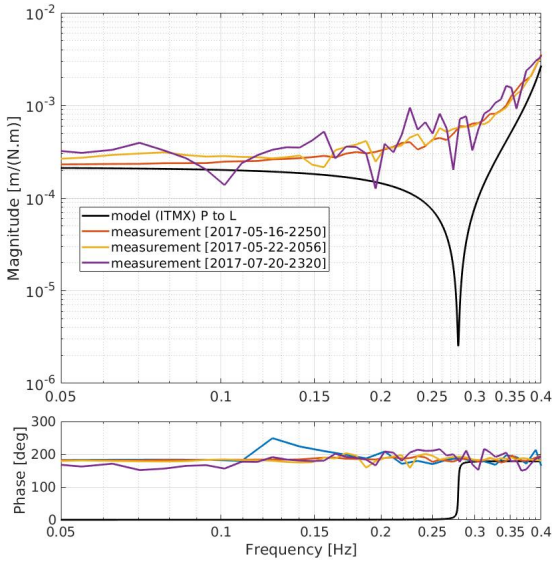

(b) H1 ITMY Top Mass Pitch to Top Mass Longitudinal transfer functions at different times during O2. Note that the traces average around -10^{-4} [1/N]